

Nuclear Repulsion Enables Division Autonomy in a Single Cytoplasm

Cori A. Anderson,¹ Umut Eser,² Therese Korndorf,¹ Mark E. Borsuk,³ Jan M. Skotheim,⁴ and Amy S. Gladfelter^{1,*}

¹Department of Biological Sciences, Dartmouth College, Hanover, NH 03755, USA

²Department of Applied Physics, Stanford University, Stanford, CA 94305, USA

³Thayer School of Engineering, Dartmouth College, Hanover, NH 03755, USA

⁴Department of Biology, Stanford University, Stanford, CA 94305, USA

Summary

Background: Current models of cell-cycle control, based on classic studies of fused cells, predict that nuclei in a shared cytoplasm respond to the same CDK activities to undergo synchronous cycling. However, synchrony is rarely observed in naturally occurring syncytia, such as the multinucleate fungus *Ashbya gossypii*. In this system, nuclei divide asynchronously, raising the question of how nuclear timing differences are maintained despite sharing a common milieu.

Results: We observe that neighboring nuclei are highly variable in division-cycle duration and that neighbors repel one another to space apart and demarcate their own cytoplasmic territories. The size of these territories increases as a nucleus approaches mitosis and can influence cycling rates. This nonrandom nuclear spacing is regulated by microtubules and is required for nuclear asynchrony, as nuclei that transiently come in very close proximity will partially synchronize. Sister nuclei born of the same mitosis are generally not persistent neighbors over their lifetimes yet remarkably retain similar division cycle times. This indicates that nuclei carry a memory of their birth state that influences their division timing and supports that nuclei subdivide a common cytosol into functionally distinct yet mobile compartments.

Conclusions: These findings support that nuclei use cytoplasmic microtubules to establish “cells within cells.” Individual compartments appear to push against one another to compete for cytoplasmic territory and insulate the division cycle. This provides a mechanism by which syncytial nuclei can spatially organize cell-cycle signaling and suggests size control can act in a system without physical boundaries.

Introduction

Classic cell-fusion experiments by Rao and Johnson from the 1970s showed that when HeLa cells in different phases of the cell cycle were fused together to form multinucleate cells, their nuclei rapidly synchronized [1–5]. Similarly, early *Drosophila* syncytial embryos orchestrate highly synchronous nuclear division cycles [6]. These findings indicate that nuclear division can be coordinated through sharing a common cytoplasm, likely by exposure to similar levels of key regulators.

Although sharing a common cytoplasm can result in synchronous nuclear division cycles, it is by no means certain. After HeLa cell fusion, nuclear asynchrony may arise in subsequent mitoses [7]. When a multinucleated myotubule re-enters the cell cycle, its nuclei do so asynchronously [8]. Similarly, many filamentous fungi display asynchronous division of nuclei in one cell [9]. Therefore, synchronization due to shared cytoplasmic signals can be spatially restricted. Although examples of asynchronous nuclear division within a common cytoplasm have been documented, the mechanisms of asynchrony in syncytia are not well understood. Asynchrony presumably requires timing variability within the nuclear division cycle in addition to a mechanism, such as compartmentalization of the cytoplasm, which would prevent adjacent nuclei from experiencing similar concentrations of regulatory molecules.

There are numerous known molecular sources of cell-cycle timing variability, including stochastic differences in gene expression and size control [10]. In *Saccharomyces cerevisiae*, stochastic expression of cell-cycle regulators generates cell-to-cell variability in division timing within a population [11, 12]. In addition, differences in cell size at birth influence the duration of G1 prior to the point of commitment to cell division [11, 13–17]. Smaller cells delay cell-cycle progression relative to larger cells, which results in timing variability within the population. In a multinucleate context, it is unknown whether nuclei sense and respond to a local volume of cytoplasm or somehow more globally coordinate nuclear division with cell growth.

Progression through the phases of the cell cycle is driven by the cyclin/CDK biochemical oscillator regulated by periodic cyclin accumulation and degradation [18–20]. In a syncytial context in which nuclei cycle asynchronously, many out-of-sync biochemical oscillators coexist and fail to entrain one another. This requires either that the activity of the oscillators (e.g., the capacity to phosphorylate substrates) is completely restricted to nuclei, perhaps due to a cytoplasmic CKI, and/or that there are barriers to diffusion of CDK activity. Such barriers would allow each nucleus to have its own segment of cytoplasm driving only its local oscillator. It is unclear what the cell biological basis would be of such cytoplasmic barriers, yet the phenomenon of asynchrony likely requires some insulation of nuclei from signaling molecules diffusing from neighboring regions.

To examine the mechanisms of asynchrony, we observe nuclear division timing and spatial distributions in the multinucleate fungus *Ashbya gossypii*. Neighboring *Ashbya* nuclei can be in different cell-cycle stages, and their nuclear division cycle times can vary widely [21]. Asynchrony in *Ashbya* emerges early in G1 and is under genetic control, as mutant cells lacking central components of the G1/S regulatory pathway become more synchronous in their division cycles [22]. Components of this pathway control transcription, which is of interest given that transcripts are translated and shared in the common cytoplasm. The importance of this transcriptional regulatory pathway for asynchrony supports the hypothesis that there may be restricted sharing of newly made proteins between neighboring nuclei. Here, we employ live-cell imaging

*Correspondence: amy.gladfelter@dartmouth.edu



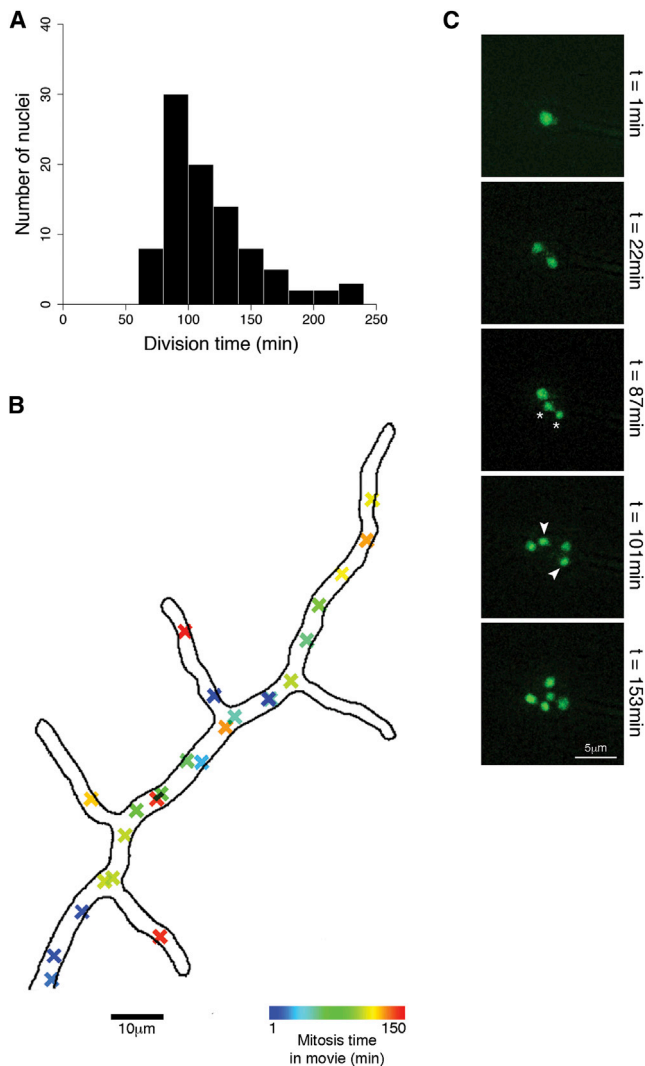


Figure 1. Mitosis in *A. gossypii* Is Not Restricted in Space or Time
(A) Observed division times in *A. gossypii* cells, mean = 118 ± 38 min ($n = 92$ division times, seven independent time-lapse movies).
(B) Plot of mitosis locations throughout the cell. Each mitosis is indicated as an “x.” The color of the “x” corresponds to the time point of mitosis. This mitosis map shows most nuclei divide in the central parental hypha rather than in the lateral side branches. Some of this bias is from the fact that the parent hypha has been in existence for longer time than the side branches, and so by chance more mitoses would occur in that region of the cell.
(C) Movie still images of dividing nuclei in a germinating spore. After the first nuclear division, sister nuclei cycle asynchronously, 15 min apart (asterisks indicate the first sister mitosis, and arrowheads indicate the second sister mitosis).
 See also [Figures S1](#) and [S4](#) and [Movies S1, S2, S3, and S4](#).

and statistical approaches to investigate how *Ashbya* nuclei functionally insulate themselves to produce variable nuclear division cycle times within a common cytoplasm.

Results

Nuclei Divide throughout Time and Space

The positions and divisions of all nuclei in single *Ashbya* cells were tracked through time using time-lapse imaging of cells expressing histone H4-GFP (*HHF1-GFP*) to visualize nuclei

([Movies S1, S2, and S3](#) available online). Nuclear coordinates were imported into MATLAB to analyze the timing patterns and spatial relationships of individual nuclei ([Movies S1, S2, and S3](#)). The mean and SD of nuclear division time were 118 and 38 min, respectively ($n = 92$ division times from seven independent time-lapse movies), consistent with previous observations ([Figure 1A](#)) [21]. Mitoses occur at all locations throughout the cell and are not restricted to a single region, such as a tip ([Figure 1B](#)), indicating that there are not stable or persistent sites that consistently favor or disallow nuclear division. Additionally, nuclei that divide around the same time point in the movie are not generally found to be near each other in the cell, indicating that there are not transient, local bursts of mitotic activity ([Figures 1B and S1](#); $n = 95$ mitoses in three independent movies). Nuclear autonomous division occurs regardless of the size of the cell. In fact, even the very first nuclear divisions after germination are asynchronous ([Figure 1C](#) and [Movie S4](#); $n = 25$ mitoses in five independent movies). These data indicate that nuclear autonomy is not a consequence of the gradual accumulation of timing differences among many nuclei as cells age and become large. Thus, regardless of overall cell size, nuclei are highly variable and asynchronous in division timing even when sharing the same cytosol.

Nuclei Are Nonrandomly Spaced Due to Microtubule-Dependent Fluctuations

How might nuclei establish functionally autonomous zones in a common cytoplasm? Notably, we see regular spacing between neighboring nuclei that is significantly different from what would be expected if they were randomly positioned ([Figures 2A and 2B](#); observed mean = $4.3 \pm 2.1 \mu\text{m}$, $p < 0.001$, Kolmogorov-Smirnov [K-S] test and F test). This prompted us to ask how nonrandom spacing is achieved and to look at how nuclei move relative to their neighbors. First, we examined nuclear positions in a variety of mutants lacking microtubule motors or having perturbed microtubule length [23–25]. The majority of these mutants show nuclei that are closer together, while cells lacking *Ase1*, a microtubule-associated protein (MAP), and the kinesin *Kip2* both show larger distances between neighboring nuclei ([Figure 2C](#) and [Table 1](#)). Importantly, the nuclear spacing in all mutant strains except *Kip2* is more variable compared to the wild-type (WT; [Table 1](#)). This increased variability is associated with nuclear spacing that is significantly more random for all mutants except *Kip2* as compared to the notably nonrandom spacing observed in the WT ([Figures 2D, 2E, and S2](#)). Thus, regulation of the microtubule cytoskeleton is critical for nonrandom nuclear spacing.

Next, we looked at how neighboring nuclei move relative to one another to examine how nonrandom spacing is achieved. To do this, we measured the difference in the distances between a nucleus and its two nearest neighbors (“neighbor offset”) and plotted the offsets through time ([Figures 3A and 3B](#)). In WT cells, the distances between individual nuclei and their neighbors typically fluctuate around a mean value; however, these fluctuations are eliminated when microtubule dynamics are impaired with nocodazole ([Figure 3C, left](#)). To further assess how neighboring nuclei change positions through time, we plotted the neighbor offset at each time point against the change in neighbor offset at the subsequent time point ([Figure 3C, middle and right](#)). In WT cells, we see that offsets change substantially each time point, as indicated by spread of points around zero. In contrast, in the absence of microtubules, nuclei no longer fluctuate in position relative to

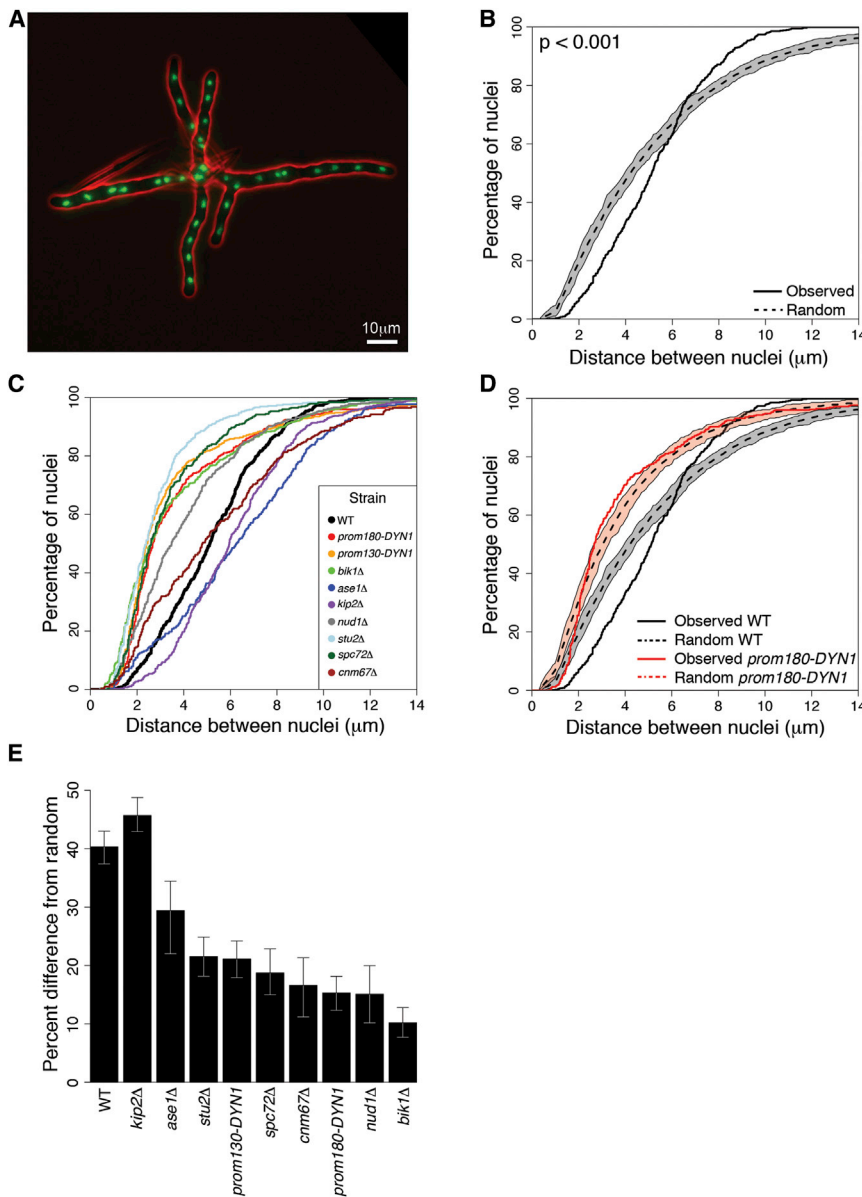


Figure 2. Nonrandom Nuclear Spacing Requires Microtubule Regulation

(A) Image of an *A. gossypii* cell expressing H4-GFP. Cell outline is false colored red.

(B) Cumulative distribution plot of observed distances between nuclei (black line) compared to randomized simulations of nuclear spacing ($p < 0.001$). The gray dashed line represents the simulated median, and the gray shaded area represents the outer bounds of 100 random simulations.

(C) Cumulative distribution plot of observed distances between nuclei in mutants that lack microtubule motors or have perturbed microtubule length.

(D) Cumulative distribution plot of observed distances between nuclei compared to a simulation of randomized nuclear spacing for both the WT and *prom180-DYN1*.

(E) Percent difference of observed nuclear spacing from random spacing. Bar heights correspond the mean of comparisons against 100 random simulations and error bars represent the 2.5th and 97.5th percentiles of these comparisons. Values near 100% indicate more constant spacing, while values near 0% indicate spacing that is closer to random.

See also [Figures S2 and S5](#), [Table S1](#), and [Movies S1, S2, S3, and S4](#).

while the cytoplasm expands due to cell growth? Importantly, all expansion is happening at hyphal tips, so most nuclei are tens to hundreds of micrometers away from the actual site where cell size is increasing, yet they maintain consistent spacing at all locations. We hypothesized that nuclear dynamics may also promote the distribution of spacing in a cell with asymmetric growth and that each nucleus could locally control the amount of space it accrues. In this model, the sizes of individual nuclear territories may change, analogous to how a uninucleate cell grows through its cell cycle.

their neighbors. In cells with depolymerized microtubules, the offsets cluster at a nonzero point, indicative of aberrant spacing, and, importantly, there is little change in the offset from time point to time point such that the points are often highly clustered ([Figure 3C](#), middle and right).

We next assessed the time scale of the fluctuations characteristic of WT cells. Autocorrelation analysis of nuclear offset over time reveals that nuclei are repelling one another on a time scale of ~ 2.2 min ([Figure 3D](#)). The autocorrelation function fits well to an exponential decay. This is consistent with an Ornstein-Uhlenbeck model for Brownian motion subject to a restoring force in a highly damped media [26]. Thus, nuclei use microtubule-based motion to repel their neighbors to produce a nonrandom spatial distribution.

Nuclei Control and Can React to Local Spacing

We hypothesize that repulsive forces between nuclei help them to subdivide the cytoplasm into “territories” or zones of influence. How then is regular nuclear spacing maintained

By tracking how neighbor spacing changes over the division cycle, we found that an increase in local spacing occurs gradually in anticipation of mitosis ([Figure 4A](#); $r = 0.91$). This growth in territory size is characteristic of most of the population, as territory size versus time yields $r > 0.5$ in 59% of nuclei ([Figures S3A and S3B](#)). Nuclei are also significantly farther from their neighbors prior to mitosis than throughout the remainder of the cell cycle ([Figure 4B](#); $p < 0.001$, K-S test). Importantly, because all cell growth is restricted to the hyphal tip, the increase in local cytoplasm size prior to mitosis is due to repositioning of nuclei and not local intercalary growth. Furthermore, because nuclei can bypass one another and migrate far from their birth location in the cell ([Figure S3C](#)), the local decrease in nuclear spacing that must occur for each mitosis is quite transient and not creating an artificial increase in space throughout the entire cell cycle. This link between the division cycle and territory size increase further supports that spacing is controlled at the level of the individual nucleus.

Table 1. Summary Statistics for Internuclear Distances

Strain	Mean (μm)	SD (μm)	CV (%)	SE of CV (%)	CV Difference from the WT (%)	Index of Dispersion	n
WT (AG523)	5.32	2.27	43.34	1.17	–	0.98	684
<i>prom180-</i> <i>DYN1</i> (AG521)	3.88	3.10	79.88	2.75	184	2.47	422
<i>prom130-</i> <i>DYN1</i> (AG522)	3.72	3.62	97.23	2.77	224	3.52	614
<i>bik1Δ</i> (AG541)	3.71	3.07	82.62	2.42	191	2.53	583
<i>ase1Δ</i> (AG545)	6.42	3.32	51.63	2.10	119	1.71	303
<i>kip2Δ</i> (AG552)	6.22	2.61	42.02	1.26	97	1.10	557
<i>nud1Δ</i> (AG559)	4.17	2.79	66.78	2.32	154	1.86	414
<i>stu2Δ</i> (AG560)	2.88	2.00	69.28	2.39	160	1.38	420
<i>spc72Δ</i> (AG561)	3.33	2.29	68.66	2.35	158	1.57	427
<i>cnm67Δ</i> (AG565)	5.89	6.03	102.36	4.11	236	6.17	310

In most uninucleate cells, cell size is inversely proportional to cycle time, so we next asked whether division timing is affected by the amount of space a nucleus inhabits at birth. However, nuclear spacing in the early period of the cycle only very weakly correlates with overall division cycle length (Figure S3D; $r = -0.19$). Additionally, nuclear spacing immediately preceding mitosis has a modest correlation with division timing (Figure S3E; $r = 0.28$). Therefore, the amount of space a nucleus is born into and ultimately possesses seems to only modestly influence overall division timing. As an additional method to investigate how territory size may be linked to division time, we artificially increased the local spacing around nuclei using nocodazole, which arrests the nuclear cycle while still allowing normal cell growth (Figures 4C and 4D). Upon release from the arrest, nuclei re-enter the division cycle, and cell growth continues at hyphal tips at normal rates (data not shown). Remarkably, we see that nuclei swiftly recover to near-WT spacing even while the cells continue to grow during the release period (Figures 4C and 4D). Therefore, the nuclear cycle must speed up in response to the increased amount of cytoplasm per nucleus to restore the original spacing. This argues that the division cycle is able to respond to alterations in the amount of cytoplasm per nucleus, but this reaction is not readily detectable unless spacing is substantially perturbed.

Nonrandom Nuclear Spacing Is Required for Division Asynchrony

The data thus far are consistent with the model that nuclear movement generates nonrandom spacing and that this functions to maintain a constant balance of nuclei to cytoplasm. We hypothesized that controlled spacing may provide insulation between neighboring nuclei to promote autonomous nuclear division. To investigate whether spacing influences the degree of asynchrony, we took advantage of a subpopulation of nuclei that undergo “bypassing” events in which they change places with one of their neighbors (Figure 5A). Such encounters require nuclei to pass $<0.25 \mu\text{m}$ from one another and thus would represent the greatest opportunity for intermingling of cell-cycle regulators. We asked whether nuclei

that came close together like this were subsequently synchronized such that they would tend to divide at the same time point of the movie. In fact, we see that nuclei that undertake a bypassing event are significantly more likely to divide at a similar moment in time than nuclei from the same data sets that are paired randomly irrespective of spacing (Figure 5B). Whereas persistent nuclear neighbors, defined as those that spend at least 30 min between 2 and 5 μm of each other yet do not bypass (Figure 5A), are more similar to the random distribution (Figure 5B; ANOVA, $p < 0.05$; median $\Delta t_{\text{p}_{\text{random}}} = 49$ min; median $\Delta t_{\text{p}_{2-5 \mu\text{m}}} = 41$ min; $\Delta t_{\text{p}_{0.25 \mu\text{m}}} = 30$ min). This suggests that nuclear spacing is important to insulate nuclei from their neighbors and to allow for nuclear cycle timing autonomy.

If controlled nuclear spacing insulates nuclei, we predict that randomly spaced nuclei would divide more synchronously than the WT. Indeed, we see a significant increase in local synchrony in cells with randomized and closer nuclear spacing due to diminished dynein expression (Figure 5C, Table 2, and Movies S5, S6, and S7). Mitoses are more likely to be adjacent to one another even though the overall proportion of dividing nuclei of this mutant strain is not substantially different from the WT (Table 2). In these cells, multiple neighboring nuclei are seen to divide at the same time and we observe “runs” of mitoses within a few time points (Figure 5C). Immunofluorescence quantification shows that there are frequent runs of nuclei in the same cell-cycle phase, with lengths of up to 12 synchronized nuclei in a row. This is in contrast to WT cells, which have fewer runs of synchronized nuclei and a frequency of such runs that is consistent with what is expected by chance (Figure 5D). These data suggest that nonrandom nuclear spacing is a key component of asynchronous nuclear division.

Sister Nuclei Inherit Nuclear Division Timing

Nuclear spacing functions to promote autonomy in nuclei, yet there is still a large amount of variation in timing across the overall population (Figure 1A). We next sought to address whether the source of timing variability is stochastic or systematic in nature. If there is some heritable or systematic source of timing variation, it should reveal itself as a timing relationship within lineages of related nuclei. Alternatively, if timing is purely stochastic, then related nuclei will have no relationship in their timing. Statistical analysis of division timing differences within and between nuclear lineages can be used to identify the existence of inherited sources of division timing variability (Figure 6A).

We examined division timing in 32 pairs of sister nuclei, born of one mitosis, from seven movies (Figure 6B and Movies S1, S2, and S3). To examine sister timing relationships, we compared the difference in nuclear-division-cycle durations of sister nuclei to a distribution of randomly selected pairs of nuclei. The mean difference between sister nuclear-cycle durations was only 23 ± 22 min compared to 41 ± 37 min for the randomized control, indicating a significant degree of inherited variation, as sisters were more similar in timing than expected by chance (Figure 6B and Table 3; $p < 0.05$, two-sample t test and K-S test). As an alternative method, we used a nonparametric rank-based statistical test to determine how sisters are related in division times and find a clear positive association (Table 3; $Z_R = 2.83$, $p < 0.01$). This also indicates that sister division times are more similar to one another than compared to the entire population of division times. Although statistically similar, sisters still have different absolute times, indicating that they are not perfectly

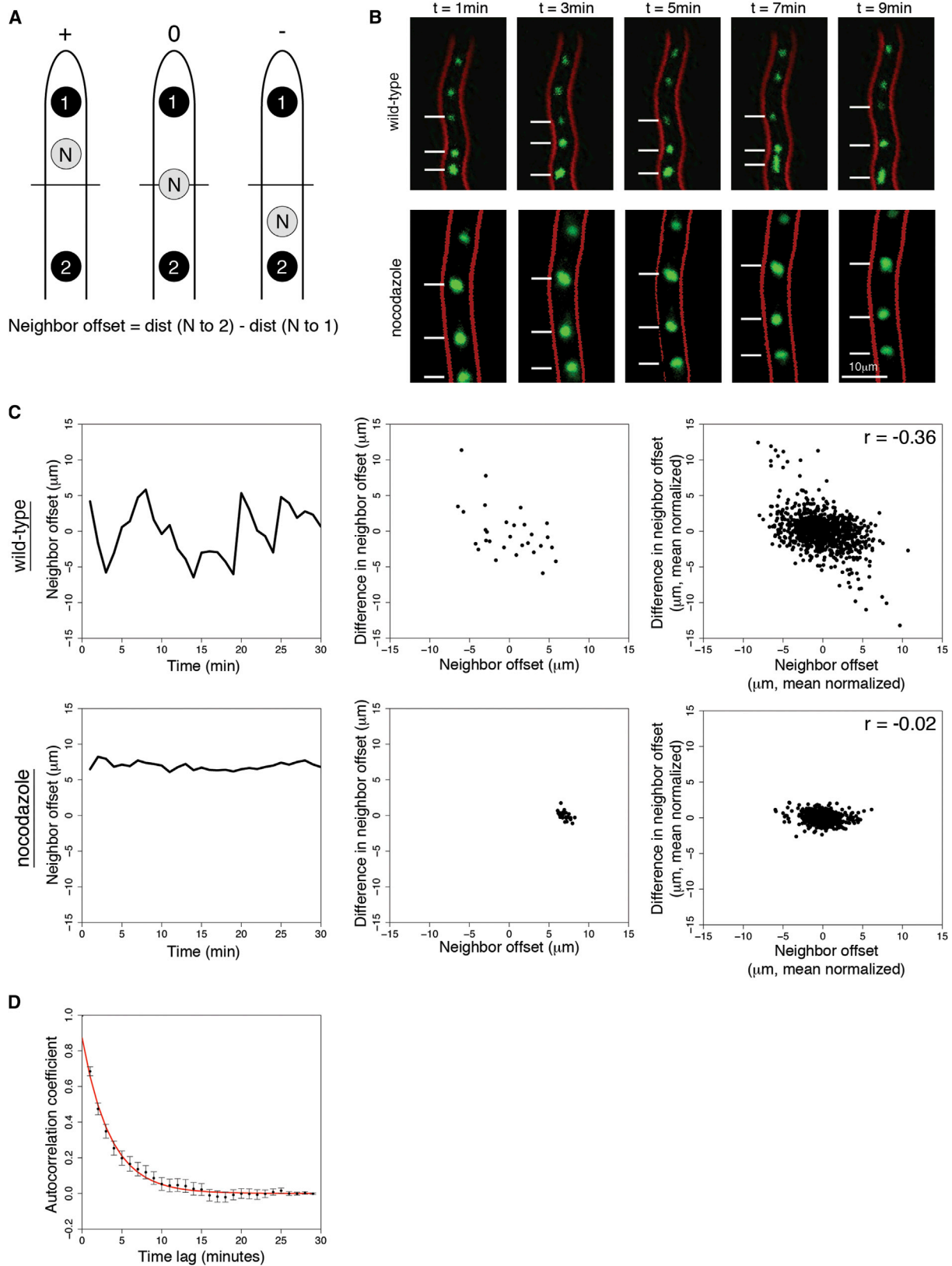


Figure 3. Nuclei Repel One Another to Generate Nonrandom Spacing

(A) Schematic of neighbor offset. The reference nucleus (N) is in gray, and its two neighboring nuclei are labeled 1 and 2. The neighbor offset for each scenario is indicated above the hypha (+, 0, or -).
 (B) Images of nuclear positions in WT and nocodazole-treated cells. Lines indicate nuclear positions of three neighboring nuclei changing over time in WT but remaining comparable in nocodazole-treated cells.

(legend continued on next page)

synchronized but rather are more similar to one another in timing than are other unrelated nuclei. These data support that a proportion of timing variability arises from a trait that is inherited by sister nuclei at mitosis and differs among the population of mitotic nuclei.

To assess whether the timing association between sisters decays as they travel far apart, we examined how far sister nuclei move away from one another after mitosis. We found that most sisters traveled away from one another, with greater than 53% of sister pairs at least 10 μm (approximately two to three nuclei) apart 75 min after their birth (Figure 6C). Additionally, sisters that travel far apart are related in timing comparably to sisters that stay in close proximity, indicating that the sister timing relationship is not strongly related to how close together they are in their next cycle, at least on the scale of tens of microns (t test, time difference of sister pairs <10 μm compared to sisters >10 μm apart, $p < 0.18$). Thus, inherited similarity in division timing is retained even when sisters are physically far apart. This inherited timing similarity is an especially robust timing determinant because it is detectable in spite of the fact that sisters undergo several bypassing events with nuclei of other lineages that would presumably diminish their association in timing (Figure 5B). This suggests that nuclei inherit regulators of division and the fact that timing is carried across distances supports the model that each nucleus creates functionally insulated territories within a seemingly continuous cytoplasm.

Discussion

Asynchrony in division timing is a universal property of cultured cells and can be observed even among cycling nuclei in a common cytoplasm of certain syncytia. Variation and autonomy in division timing may protect against external stress, e.g., by limiting the number of nuclei during the sensitive state of DNA replication. Additionally, they may serve to maintain a consistent nuclear-to-cytoplasmic ratio. Therefore, there are likely to be active mechanisms that promote asynchrony in multinucleate contexts. We analyzed nuclear asynchrony in *Ashbya* by considering two different division cycle timing relationships: (1) nuclei that are neighbors and (2) sister nuclei that are born of one mitosis and then move far apart from one another. We hypothesized that nuclei may generate independent compartments of cytosol that foster division autonomy. Consistent with this idea, we found that nuclei in the *Ashbya* syncytium are nonrandomly distributed and actively repel neighbors to generate nuclear territories or “cells within cells.” Cytoplasmic territories respond to the local nuclear division cycle and are likely to be a mechanism by which nuclear density is coordinated with overall cell growth. Thus, active nuclear positioning promotes nuclear autonomy and asynchronous division of neighboring nuclei.

Nuclear spacing is critical in many organisms for diverse cellular functions and cellular organization [27]. We have evidence that nuclei actively control their spacing relative to neighbors in *Ashbya* using nuclear repulsion and microtubules (Figures 2 and 3). Previous work in *Ashbya* has shown that

nuclei utilize the microtubule cytoskeleton to fluctuate and bypass within the common cytoplasm [23, 25, 28, 29]. In addition, small data sets have shown neighboring nuclei moving close to one another and then rapidly moving apart and being carried by cytoplasmic flow [30]. Our analyses of large populations of dynamic nuclei support these findings and indicate that individual nuclei create territories by controlling local cytoplasmic spacing. We observe that nuclear positions fluctuate about a mean position and that nuclei are pushed back to the mean on a time scale of ~ 2.2 min by a microtubule-dependent mechanism (Figure 3). Similar nuclear fluctuations, which begin after nuclear fusion in meiosis in *S. pombe*, are controlled by dynein motors. The asymmetric loading of dynein and the dynamic redistribution of dynein on microtubules due to load forces facilitate these oscillatory movements. These horsetail oscillations occur with an ~ 10 min period and span a 10 μm distance, which is a relatively similar time and length scale as we see in *Ashbya* [31]. We speculate that spatially variable regulation of dynein localization and activity in *Ashbya* is likely to be the basis of nuclear repulsion and nonrandom nuclear positioning.

The observation that local nuclear spacing increases with progression through the nuclear-division cycle suggests that the nuclear-division cycle is in fact able to act on cytoplasmic targets to regulate local nuclear crowding. Local nuclear-division-cycle regulation of microtubule-associated proteins or motors may function to alter local nuclear spacing as nuclei progress through their cycle. Overlapping microtubules emanating from neighboring nuclei may be responsible for nuclear repulsion [28]. Short cytoplasmic microtubules are thought to generate forces that may be resisted by some other component of the cytosol that perhaps changes stiffness with the cell cycle and allows for MT motors to work [23, 29, 32]. Interestingly, there is evidence that aster-aster interaction zones, such as those seen in the early divisions of large cells such as zebrafish and *Xenopus* embryos, are also spaced apart depending on when in the cell cycle the asters meet. This spacing is speculated to be based on dynein activity from molecules anchored on the cytosol [33, 34]. Regulation of motor activity may enhance the pushing apart of neighboring nuclei in preparation for mitosis in *Ashbya*, and several motors examined in our study have consensus CDK phosphorylation sites. The identity of the cytosolic substrates reacting to this regulation in *Ashbya* and how this regulation would be spatially restricted to a zone of single nucleus requires further investigation.

There is mounting evidence for cytoplasmic organization within many syncytia. Crosses of *Neurospora crassa* “banana” mutants generate one large multinucleate ascospore with a genetically mixed population of nuclei. When banana mutant crosses involve one parent strain expressing GFP, those nuclei that encode GFP have increased GFP localization compared to nuclei from the parent without the fluorescent label encoded, even though the nuclei reside in a common cytoplasm. This pattern is accentuated after several mitotic divisions, resulting in a gradient of GFP intensity from one end of the spore to the other, a distance of approximately 100 μm [35]. Nuclear-based cytoplasmic organization has

(C) Nuclear offset time series for WT cells and nocodazole-treated cells. Left plots: neighbor offset through time for an individual nucleus. Middle plots: scatterplot of neighbor offset versus difference in neighbor offset for a single nucleus. Right plots: mean normalized neighbor offset versus difference in neighbor offset for all tracked nuclei.

(D) Autocorrelation functions of nuclear offsets in WT cells and an exponential fit (red). Points represent mean autocorrelation function over all WT nuclear traces; error bars represent the SEM.

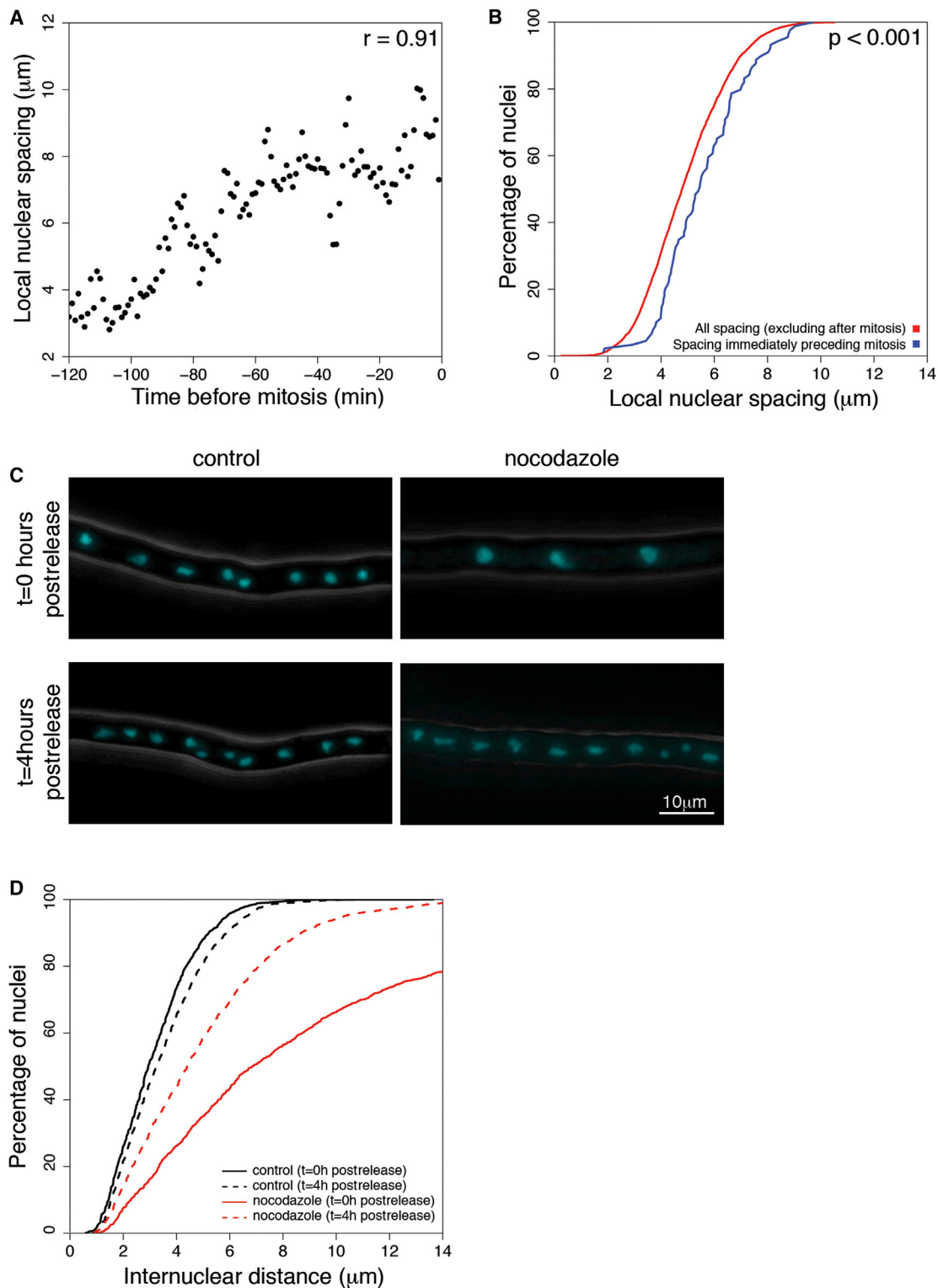


Figure 4. Local Nuclear Spacing Is Related to Cell-Cycle Progression

(A) Scatterplot of local nuclear spacing through time for an individual nucleus ($r = 0.91$).

(B) Cumulative distribution plots of all nuclear spacing (excluding time points immediately after mitoses) and spacing immediately before a mitosis event.

(C) Still images of nuclear spacing at $t = 0$ hr and $t = 4$ hr after nocodazole treatment release. Cells were treated with either dimethyl sulfoxide (DMSO) or $10 \mu\text{g/ml}$ nocodazole for 4 hr before release.

(D) Cumulative distribution plot of internuclear distances at $t = 0$ hr and $t = 4$ hr after release. Cells were treated with either DMSO or $10 \mu\text{g/ml}$ nocodazole for 4 hr before release. $t = 0$ hr postrelease: control median = $2.9 \mu\text{m}$, nocodazole median = $6.9 \mu\text{m}$. $t = 4$ hr postrelease: control median = $3.2 \mu\text{m}$, nocodazole median = $4.4 \mu\text{m}$.

See also [Movies S1](#), [S2](#), [S3](#), and [S4](#).

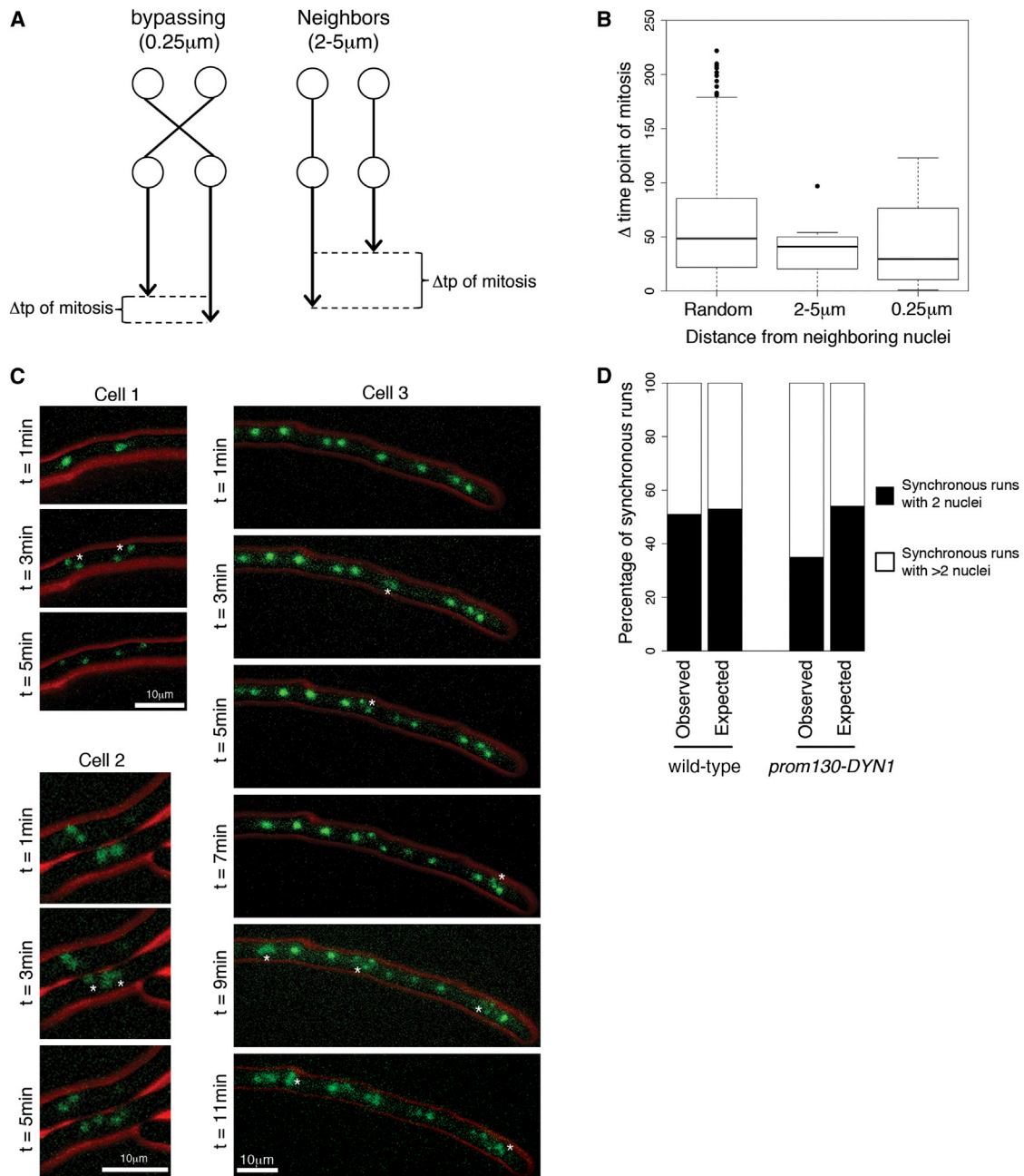


Figure 5. Nuclear Spacing and Division Timing Synchrony

(A) Schematic of nuclear relationships. Bypassing nuclei are defined as those that come within 0.25 μm of each other. Neighboring nuclei are defined as those who spend >30 min within 2 to 5 μm of each other. The difference between the time point of division for each nuclear relationship is indicated as Δ time point of mitosis.

(B) Box plot of Δ time point of mitosis for all tracked nuclei and observed divisions. A randomized Δ time point was calculated based on observed mitosis times. ANOVA, $p < 0.05$.

(C) Movie still images of nuclei in *prom130-DYN1* cells. Synchronously dividing nuclei are indicated with an asterisk (*). In cells 1 and 2, neighboring nuclei divide at the exact same time, while a run of several nuclei in cell 3 divide within a 10 min time span.

(D) Stacked bar plot of synchronous runs of nuclei based on immunofluorescence analysis of cell-cycle stages. Black bars indicate those runs that contain only two nuclei, and bars in white represent those runs with three or more nuclei. A chance proportion of expected runs was calculated and plotted to compare with the observed synchrony in both the WT and *prom130-DYN1*. See also Figure S3, Table S1, and Movies S1, S2, S3, S4, S5, S6, and S7.

also been observed in the *Drosophila* syncytial embryo that contains thousands of nuclei in one cytoplasm and, prior to cellularization, endomembranes (endoplasmic reticulum and Golgi) are organized to create functionally distinct units around individual nuclei [36–38]. These examples, when combined

with this study, support that nuclei can insulate themselves within a common cytoplasm.

The notion that individual nuclei in a syncytium may be in conflict or competition, which we observe as the repulsion of nuclear neighbors from one another, is well documented on

Table 2. Synchrony Index

Genotype	Cell-Cycle Stages (%)			Observed Synchrony (%)	Chance Synchrony (%)	Synchrony Index
	G1	S/G2	M			
WT	52	35	13	48	41	1.16
<i>prom130-DYN1::GEN3</i>	48	44	8	62	43	1.45 ^a

^aSignificantly different than the WT synchrony index ($p < 0.03$).

the genetic level. Individual genomes in filamentous fungi can give rise to new individuals through asexual spore formation, and there is substantial thought and interest considering the role of nuclear migration and position in the potential for intracellular genome competition [39]. Our ability to detect independence of nuclear movement coupled to functional insulation adds support to the idea that there can be functionally relevant genome competition even in a common cytoplasm.

While mitosis in *Ashbya* is not restricted in time and space and overall division time is highly variable (Figure 1), sister nuclei have related division timing even when traveling apart after their birth (Figure 6). These surprising results suggest that timing variability arises from a trait that is inherited by sister nuclei at mitosis and differs among the population of mitotic nuclei. Due to limitations of phototoxicity and tracking, it is not possible to determine from these data whether similar division times persist in a lineage over many generations. However, if timing were inherited consistently over multiple generations, we predict that the mean division timing for a population of nuclei would decrease as the cells age. In fact, we observe that mean division timing increases as the cells age, suggesting that the persistence of division timing within a lineage of related nuclei is short (data not shown). The molecular basis for the shared timing behavior is not yet clear but could lie in the transcriptional state, ploidy, and/or the distribution of nuclear pore complexes which are all traits that are known to vary between nuclei in *Ashbya* (unpublished data).

As in uninucleate cells, one of the sources of timing variation in *Ashbya* nuclear division cycles is the size of the local cytoplasm [17, 40–44]. There is evidence for local size control working in the multinucleate context of fused onion root cells, where the nuclei with persistent access to a larger area of the cytoplasm progress through prophase earlier than those that are more crowded [45]. The modest correlation between nuclear spacing and cell-cycle progression we observe in *Ashbya* suggests that territory size may have some influence on division timing (Figure S3). It is likely that local nuclear spacing is more clearly important for the duration of specific phases of the cell cycle; our data analyze complete division-cycle times because G1 and G2 durations are unknown in this data set. Thus, strong evidence for size control of cell-cycle progression, particularly early in the division cycle, may be obscured by sources of timing variability acting in other phases of the cycle.

Importantly, we found that large alterations in nuclear spacing clearly resulted in an increased mitosis rate (Figures 4C and 4D). This suggests that the cell is able to sense and respond to the amount of cytoplasm associated with each nucleus. Prior to this work, genetic evidence for controlling the amount of cytoplasm per nucleus in *Ashbya* included the fact that the internuclear distances get smaller in certain cell-cycle mutants (such as *whi5*) known to accelerate G1 [22]. This change in nuclear spacing in *Ashbya* mutants is

analogous to budding and fission yeast mutants altering G1/S and G2/M control, respectively, leading to overly small or large cells [46–49]. While the relative amount of cytoplasm around a nucleus can contribute to nuclear division cycle timing, the mechanism for such size control is unclear. Some mechanisms proposed for budding yeast to measure size, such as the measurement of local protein synthesis rate may be applicable in both uninucleate and syncytial cells [10].

Nuclear positioning allows *Ashbya* to create “cells within cells” to foster autonomy. We observed that altering the nuclear spacing results in increased synchrony across the cell. When nuclei are more randomly spaced, neighboring nuclei are more likely to be in the same cell-cycle stage and are seen to undergo mitosis at the same time (Figure 5, Table 2, and Movies S5, S6, and S7). This suggests that nuclei are no longer able to compartmentalize themselves relative to their neighbors and are potentially more able to share diffusing signaling molecules. Supporting this hypothesis, even in WT cells we see that nuclei that come very close together are more likely to divide at the same moment of time than nuclei that are spaced apart (Figure 5). Thus, nonrandom nuclear spacing is critical for cell-cycle independence within the syncytium.

Given that the cell-cycle machinery acts in the cytoplasm, as evidenced by spacing increasing with nuclear progression, how are nuclear territories supporting division autonomy? What is the basis for individuality of nuclear compartments within a single cell? Proteins must be translated in the common cytoplasm and yet be restricted to act in or near individual nuclear territories. We have evidence that some cyclin transcripts are preferentially sequestered near nuclei and this could lead to local translation and influence over the most proximal nucleus [50]. The cell biological basis of nuclear autonomy is fascinating and future work will assess the degree to which proteins and transcripts can be shared among neighboring nuclei, as well as additional mechanisms that are acting within nuclear territories to promote nuclear autonomy.

Experimental Procedures

Growth Conditions and Strain Construction

Ashbya gossypii media, culturing, and transformation conditions were performed as described previously [51, 52]. Details on strain construction and preparation of cells for imaging are provided in the Supplemental Experimental Procedures.

Imaging

Time-lapse imaging was performed using a Zeiss Axioimage-M1 upright light microscope (Carl Zeiss) equipped with a Plan-Apochromat 63×/1.4 NA oil objective, an Exfo X-Cite 120 lamp in conjunction with the following filters: Zeiss 38HE (GFP), Chroma 41002B (TRITC), and Zeiss 49 (Hoechst). Images were acquired on an Orca-AG charge-coupled device camera (C4742-80-12AG; Hamamatsu) driven by OpenLab 5 (Improvision) or μ Manager (NIH, [53]). Acquisition and processing details are in the Supplemental Experimental Procedures.

Nuclear Tracking

The position of each nucleus at each time point was tracked and coordinates were recorded in Excel for three time-lapse movies using the measurements tool in Volocity 5 (Improvision). Four additional movies were tracked for lineages. Subsequent spatial analyses were done in Excel and in MATLAB (see below). All statistical tests were performed in Excel or R (version 2.12.2). Data plotting was all done in R.

Simulations of Random Nuclear Positioning

For comparison of the internuclear distances observed in the mutant and WT strains to what would be expected by random nuclear positioning, a null “randomized” model was simulated in MATLAB using a Monte Carlo procedure. Maintaining the same number of nuclei in the same hyphal

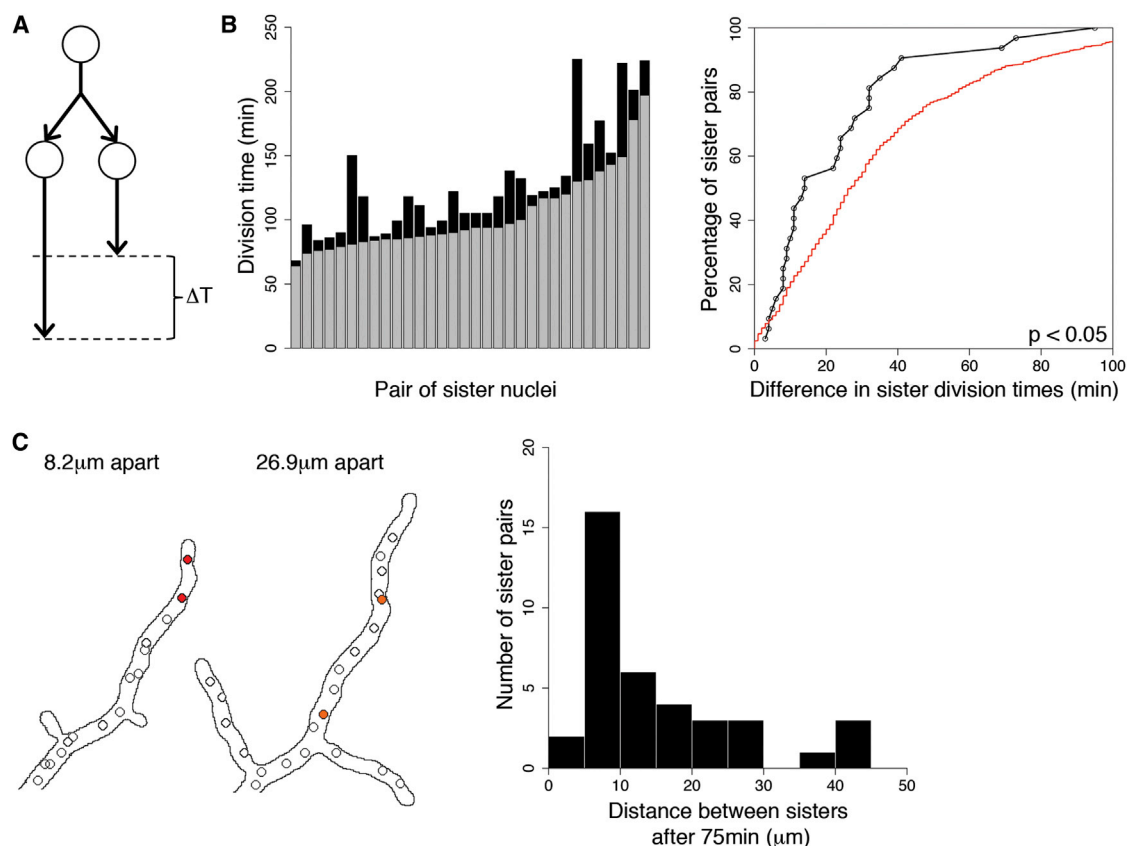


Figure 6. Sister Nuclear Division Cycle Durations Are Correlated

(A) Schematic of division timing relationship in a nuclear lineage (difference in observed division times is shown as ΔT).

(B) Sister nuclear cycle durations. The nuclear division cycle length of the slower sister is plotted in black with the faster sister overlaid in gray ($n = 32$ pairs of sisters). K-S test plot of observed sister nuclear cycle durations. The observed differences in sister division times displayed as a cumulative distribution plot in black. A randomized difference was calculated and the cumulative distribution shown as a red line ($p < 0.05$).

(C) Representative nuclear pairs that remain close or travel far apart over time (red nuclear pair is $8.2 \mu\text{m}$ apart and orange nuclear pair is $26.9 \mu\text{m}$ apart 75 min after mitosis). Histogram of sister distances 75 min after mitosis.

geometry, nuclear positions were randomly simulated 100 times per strain, and internuclear distances were calculated. By creating distinct random simulations based on the mean spacing of each mutant strain, we ensured that mutants were compared to a random distribution with the same mean, therefore avoiding artifacts of comparing distributions with different means. To indicate the degree to which the observed nuclear distances differ from random, we calculated a metric for each random simulation. This metric was based on the total area between the observed CDF and the simulated random CDF (A_{rand}), as well as the total area between the observed CDF and a CDF representing uniform spacing (A_{unif}). The utilized metric was then calculated as $100 \cdot A_{\text{rand}} / (A_{\text{rand}} + A_{\text{unif}})$ to yield a measure between 0% and 100%. Values near 100% indicate more uniform spacing, while values near 0% indicate spacing that is closer to random.

Table 3. Rank and K-S Test Statistics

	Rank Test		K-S Test		Medians, Observed (Random)
	Z_R	p Value	D	p Value	
Figure S2 simulations: negative association	-3.33	<0.001	0.19	<0.01	37.75 (25.08)
Figure S2 simulations: no association	0.38	0.35	0.08	0.65	27.42 (29.79)
Figure S2 simulations: positive association	5.57	<0.001	0.21	<0.001	16.80 (25.82)
Observed times	2.83	<0.01	0.27	<0.05	13.99 (26.99)

Neighbor Distance and Time-Point Analysis

For determination of whether close proximity between nuclei resulted in similarity in the time point of division, the distance between all tracked nuclei was calculated over time. Bypassing nuclei were those that came within $0.25 \mu\text{m}$ or less within their lifetime. For each observed mitosis, all bypassing nuclei were identified, and the average division time point of those nuclei was calculated. The absolute value of that average and the observed division time point of the reference nucleus was calculated. Neighboring nuclei were considered those that spent more than 30 time points within 2 to $5 \mu\text{m}$ of each other, excluding those nuclei that underwent bypassing events. The same analyses that were done for bypassing nuclei were done using neighboring nuclei.

A description of methods used for strain construction, image processing, nocodazole arrest and release, nuclear tracking, calculating the synchrony index and statistical analysis of sister division time relationships can be found in the [Supplemental Experimental Procedures](#).

Supplemental Information

Supplemental Information includes Supplemental Experimental Procedures, five figures, and one table and can be found with this article online at <http://dx.doi.org/10.1016/j.cub.2013.07.076>.

Acknowledgments

We would like to thank Hany Farid for computational assistance, the Gladfelter lab, Christine Field, and Tim Mitchison for discussion, and Jamie Moseley and Roger Sloboda for useful comments on the manuscript. We are grateful to MicroVideo Instruments (MVI) and Nikon for supporting our

instrument needs at MBL in Woods Hole, MA. This work was supported by NIH R01-GM081506 (A.S.G.), Lemann and Colwin fellowships (A.S.G.) from the Marine Biological Laboratory in Woods Hole, NIH award T32GM008704 (C.A.A.), NIH R01-GM092925 (J.S.), and the Burroughs Wellcome Fund (J.S.).

Received: January 28, 2013

Revised: May 31, 2013

Accepted: July 23, 2013

Published: October 3, 2013

References

1. Rao, P.N., and Johnson, R.T. (1972). Premature chromosome condensation: a mechanism for the elimination of chromosomes in virus-fused cells. *J. Cell Sci.* **10**, 495–513.
2. Johnson, R.T., and Rao, P.N. (1971). Nucleo-cytoplasmic interactions in the achievement of nuclear synchrony in DNA synthesis and mitosis in multinucleate cells. *Biol. Rev. Camb. Philos. Soc.* **46**, 97–155.
3. Rao, P.N., and Johnson, R.T. (1971). Mammalian cell fusion. IV. Regulation of chromosome formation from interphase nuclei by various chemical compounds. *J. Cell. Physiol.* **78**, 217–223.
4. Johnson, R.T., and Rao, P.N. (1970). Mammalian cell fusion: induction of premature chromosome condensation in interphase nuclei. *Nature* **226**, 717–722.
5. Johnson, R.T., Rao, P.N., and Hughes, H.D. (1970). Mammalian cell fusion. 3. A HeLa cell inducer of premature chromosome condensation active in cells from a variety of animal species. *J. Cell. Physiol.* **76**, 151–157.
6. Foe, V.E., and Alberts, B.M. (1983). Studies of nuclear and cytoplasmic behaviour during the five mitotic cycles that precede gastrulation in *Drosophila* embryogenesis. *J. Cell Sci.* **61**, 31–70.
7. Westerveld, A., and Freeke, M.A. (1971). Cell cycle of multinucleate cells after cell fusion. *Exp. Cell Res.* **65**, 140–144.
8. Cardoso, M.C., Leonhardt, H., and Nadal-Ginard, B. (1993). Reversal of terminal differentiation and control of DNA replication: cyclin A and Cdk2 specifically localize at subnuclear sites of DNA replication. *Cell* **74**, 979–992.
9. Gladfelter, A.S. (2006). Nuclear anarchy: asynchronous mitosis in multinucleated fungal hyphae. *Curr. Opin. Microbiol.* **9**, 547–552.
10. Turner, J.J., Ewald, J.C., and Skotheim, J.M. (2012). Cell size control in yeast. *Curr. Biol.* **22**, R350–R359.
11. Di Talia, S., Skotheim, J.M., Bean, J.M., Siggia, E.D., and Cross, F.R. (2007). The effects of molecular noise and size control on variability in the budding yeast cell cycle. *Nature* **448**, 947–951.
12. Bean, J.M., Siggia, E.D., and Cross, F.R. (2006). Coherence and timing of cell cycle start examined at single-cell resolution. *Mol. Cell* **21**, 3–14.
13. Doncic, A., Falleur-Fettig, M., and Skotheim, J.M. (2011). Distinct interactions select and maintain a specific cell fate. *Mol. Cell* **43**, 528–539.
14. Nash, R.S., Tokiwa, G., Anand, S., Erickson, K., and Futcher, A.B. (1988). The WHI1+ gene of *Saccharomyces cerevisiae* tethers cell division to cell size and is a cyclin homolog. *EMBO J.* **7**, 4335–4346.
15. Wheals, A.E. (1982). Size control models of *Saccharomyces cerevisiae* cell proliferation. *Mol. Cell. Biol.* **2**, 361–368.
16. Lord, P.G., and Wheals, A.E. (1981). Variability in individual cell cycles of *Saccharomyces cerevisiae*. *J. Cell Sci.* **50**, 361–376.
17. Johnston, G.C., Pringle, J.R., and Hartwell, L.H. (1977). Coordination of growth with cell division in the yeast *Saccharomyces cerevisiae*. *Exp. Cell Res.* **105**, 79–98.
18. Murray, A.W., and Kirschner, M.W. (1989). Cyclin synthesis drives the early embryonic cell cycle. *Nature* **339**, 275–280.
19. Murray, A.W., Solomon, M.J., and Kirschner, M.W. (1989). The role of cyclin synthesis and degradation in the control of maturation promoting factor activity. *Nature* **339**, 280–286.
20. Bloom, J., and Cross, F.R. (2007). Multiple levels of cyclin specificity in cell-cycle control. *Nat. Rev. Mol. Cell Biol.* **8**, 149–160.
21. Gladfelter, A.S., Hungerbuehler, A.K., and Philippsen, P. (2006). Asynchronous nuclear division cycles in multinucleated cells. *J. Cell Biol.* **172**, 347–362.
22. Nair, D.R., D'Ausilio, C.A., Occhipinti, P., Borsuk, M.E., and Gladfelter, A.S. (2010). A conserved G₁ regulatory circuit promotes asynchronous behavior of nuclei sharing a common cytoplasm. *Cell Cycle* **9**, 3771–3779.
23. Lang, C., Grava, S., Finlayson, M., Trimble, R., Philippsen, P., and Jaspersen, S.L. (2010). Structural mutants of the spindle pole body cause distinct alteration of cytoplasmic microtubules and nuclear dynamics in multinucleated hyphae. *Mol. Biol. Cell* **21**, 753–766.
24. Grava, S., Keller, M., Voegeli, S., Seger, S., Lang, C., and Philippsen, P. (2011). Clustering of nuclei in multinucleated hyphae is prevented by dynein-driven bidirectional nuclear movements and microtubule growth control in *Ashbya gossypii*. *Eukaryot. Cell* **10**, 902–915.
25. Grava, S., and Philippsen, P. (2010). Dynamics of multiple nuclei in *Ashbya gossypii* hyphae depend on the control of cytoplasmic microtubules length by Bik1, Kip2, Kip3, and not on a capture/shrinkage mechanism. *Mol. Biol. Cell* **21**, 3680–3692.
26. Gardiner, C.W. (1985). *Handbook of Stochastic Methods for Physics, Chemistry, and the Natural Sciences* (Berlin: Springer-Verlag).
27. Gundersen, G.G., and Worman, H.J. (2013). Nuclear positioning. *Cell* **152**, 1376–1389.
28. Gibeaux, R., Lang, C., Politi, A.Z., Jaspersen, S.L., Philippsen, P., and Antony, C. (2012). Electron tomography of the microtubule cytoskeleton in multinucleated hyphae of *Ashbya gossypii*. *J. Cell Sci.* **125**, 5830–5839.
29. Lang, C., Grava, S., van den Hoorn, T., Trimble, R., Philippsen, P., and Jaspersen, S.L. (2010). Mobility, microtubule nucleation and structure of microtubule-organizing centers in multinucleated hyphae of *Ashbya gossypii*. *Mol. Biol. Cell* **21**, 18–28.
30. Alberti-Segui, C., Dietrich, F.S., Altmann-Jöhl, R., Hoepfner, D., and Philippsen, P. (2001). Cytoplasmic dynein is required to oppose the force that moves nuclei towards the hyphal tip in the filamentous ascomycete *Ashbya gossypii*. *J. Cell Sci.* **114**, 975–986.
31. Vogel, S.K., Pavin, N., Maghelli, N., Jülicher, F., and Tolić-Nurelykke, I.M. (2009). Self-organization of dynein motors generates meiotic nuclear oscillations. *PLoS Biol.* **7**, e1000087.
32. Field, C.M., Wühr, M., Anderson, G.A., Kueh, H.Y., Strickland, D., and Mitchison, T.J. (2011). Actin behavior in bulk cytoplasm is cell cycle regulated in early vertebrate embryos. *J. Cell Sci.* **124**, 2086–2095.
33. Mitchison, T., Wühr, M., Nguyen, P., Ishihara, K., Groen, A., and Field, C.M. (2012). Growth, interaction, and positioning of microtubule asters in extremely large vertebrate embryo cells. *Cytoskeleton (Hoboken)* **69**, 738–750.
34. Wühr, M., Tan, E.S., Parker, S.K., Detrich, H.W., 3rd, and Mitchison, T.J. (2010). A model for cleavage plane determination in early amphibian and fish embryos. *Curr. Biol.* **20**, 2040–2045.
35. Freitag, M., Hickey, P.C., Raju, N.B., Selker, E.U., and Read, N.D. (2004). GFP as a tool to analyze the organization, dynamics and function of nuclei and microtubules in *Neurospora crassa*. *Fungal Genet. Biol.* **41**, 897–910.
36. Frescas, D., Mavrakis, M., Lorenz, H., Delotto, R., and Lippincott-Schwartz, J. (2006). The secretory membrane system in the *Drosophila* syncytial blastoderm embryo exists as functionally compartmentalized units around individual nuclei. *J. Cell Biol.* **173**, 219–230.
37. Mavrakis, M., Rikhy, R., and Lippincott-Schwartz, J. (2009). Cells within a cell: Insights into cellular architecture and polarization from the organization of the early fly embryo. *Commun. Integr. Biol.* **2**, 313–314.
38. Mavrakis, M., Rikhy, R., and Lippincott-Schwartz, J. (2009). Plasma membrane polarity and compartmentalization are established before cellularization in the fly embryo. *Dev. Cell* **16**, 93–104.
39. Gladfelter, A.S., and Berman, J. (2009). Dancing genomes: fungal nuclear positioning. *Nat. Rev. Microbiol.* **7**, 875–886.
40. Fantes, P., and Nurse, P. (1977). Control of cell size at division in fission yeast by a growth-modulated size control over nuclear division. *Exp. Cell Res.* **107**, 377–386.
41. Fantes, P.A. (1977). Control of cell size and cycle time in *Schizosaccharomyces pombe*. *J. Cell Sci.* **24**, 51–67.
42. Fantes, P.A. (1981). Division timing: controls, models and mechanisms. In *The Cell Cycle*, P.C.L. John, ed. (New York: Cambridge University Press).
43. Fantes, P.A. (1981). Cell cycle controls in fission yeast: a genetic analysis. In *The Cell Cycle*, P.C.L. John, ed. (New York: Cambridge University Press).
44. Nurse, P., and Thuriaux, P. (1977). Controls over the timing of DNA replication during the cell cycle of fission yeast. *Exp. Cell Res.* **107**, 365–375.
45. Gimenez-Martin, G., Lopez-Saez, J.F., Moreno, P., and Gonzalez-Fernandez, A. (1968). On the triggering of mitosis and the division cycle of polynucleate cells. *Chromosoma* **25**, 282–296.

46. Thuriaux, P., Nurse, P., and Carter, B. (1978). Mutants altered in the control co-ordinating cell division with cell growth in the fission yeast *Schizosaccharomyces pombe*. *Mol. Gen. Genet.* *161*, 215–220.
47. Russell, P., and Nurse, P. (1986). *cdc25+* functions as an inducer in the mitotic control of fission yeast. *Cell* *45*, 145–153.
48. Nash, R.S., Volpe, T., and Futcher, B. (2001). Isolation and characterization of WHI3, a size-control gene of *Saccharomyces cerevisiae*. *Genetics* *157*, 1469–1480.
49. Surana, U., Robitsch, H., Price, C., Schuster, T., Fitch, I., Futcher, A.B., and Nasmyth, K. (1991). The role of CDC28 and cyclins during mitosis in the budding yeast *S. cerevisiae*. *Cell* *65*, 145–161.
50. Lee, C., Zhang, H., Baker, A.E., Occhipinti, P., Borsuk, M.E., and Gladfelder, A.S. (2013). Protein aggregation behavior regulates cyclin transcript localization and cell-cycle control. *Dev. Cell* *25*, 572–584.
51. Wendland, J., Ayad-Durieux, Y., Knechtle, P., Rebischung, C., and Philippsen, P. (2000). PCR-based gene targeting in the filamentous fungus *Ashbya gossypii*. *Gene* *242*, 381–391.
52. Ayad-Durieux, Y., Knechtle, P., Goff, S., Dietrich, F.S., and Philippsen, P. (2000). A PAK-like protein kinase is required for maturation of young hyphae and septation in the filamentous ascomycete *Ashbya gossypii*. *J. Cell Sci.* *113*, 4563–4575.
53. Edelstein, A., Amodaj, N., Hoover, K., Vale, R., and Stuurman, N. (2001). Computer Control of Microscopes using μ Manager (Hoboken: John Wiley & Sons, Inc.).